

Copyright 2016, ABRACO

Trabalho apresentado durante o INTERCORR 2016, em Búzios/RJ no mês de maio de 2016.

As informações e opiniões contidas neste trabalho são de exclusiva responsabilidade do(s) autor(es).

LEGENDA:

Influence of small amount of H₂S on the CO₂ corrosion of carbon steel at oil production conditions

Merlin C. E. Bandeira^a, Danielle Spigarollo^b, Rogaciano M. Moreira^c, Oscar R. Mattos^d

Abstract

The corrosion of carbon steel at pre-salt oil production conditions was investigated in order to evaluate the influence of 100 mg/L of H₂S on CO₂ corrosion of X65 carbon steel at 10MPa, 100°C and 150,000 ppm of Cl⁻. All the tests were performed at supercritical conditions. It was also compared results of stagnant, intermediate and high shear stress corrosion tests. Electrochemical measurements, weight loss tests, surface analyses by Scanning Electronic Microscopy (SEM) and X-ray diffraction were performed to better understand the corrosion process. The results of this work showed high corrosion rates to all conditions studied, reaching up to 41,9 mm/y for 50 Pa in the presence of H₂S. Under stagnant conditions the corrosion rates were lower, but with relatively high values, 6,13 mm/y in the H₂S medium. In all tested conditions, the H₂S increased the carbon steel corrosion rates. It was also observed that the corrosion rates increased to higher shear stress. X-ray and SEM analyses confirmed the presence of FeCO₃ and Fe₂O₂CO₃ layers on static tests and FeCO₃ for dynamic tests. The impedance diagrams for all conditions clearly show the influence of H₂S on film formation and consequently on corrosion rates.

Keywords: CO₂, H₂S, corrosion, pre-salt

Introduction

Each year, the oil companies spend large sums in order to prevent or mitigate CO₂ and H₂S corrosion that can lead to structural failures, especially on pipelines/flowlines, causing downtime, human accidents and environmental hazards. Gases such as CO₂ and H₂S are present during production and oil processing. These gases react in contact with water decreasing the pH, which increases the corrosiveness of the medium. The role of those gases in the corrosion process is under discussion in the literature (1-5).

Carbon dioxide reacts with water producing carbonic acid, and its dissociation decrease the pH favoring corrosion and produces other chemical species, HCO₃⁻ and CO₃²⁻. High corrosion

^a Ph.D, Material Science – LNDC Researcher

^b MSc., Chemical Engineer – UFRJ/LNDC

^c Ph.D, Physical Chemistry – LNDC Researcher

^d Ph.D, Physical Chemistry – Prof. POLI/COPPE/UFRJ

rates are often registered when carbon steel is exposed to environments with CO₂. Those corrosion rates are usually proportional to CO₂ partial pressure and temperature (6,7). Similar to CO₂, the H₂S dissolved in water produces HS⁻ and S²⁻ species, decreasing the pH and increasing the corrosion process. Consequently, the dissociation of the weak acid will be activated adjusting the pH in the previous acid value and accelerating the overall corrosion process. However, all those chemical species together with Fe²⁺ generated by the steel corrosion may form and iron carbonate and/or iron sulfide films on the steel surface that somehow diminishes the steel corrosion. Therefore, film formation plays a key role on carbon steel corrosion rates once they act as barriers decreasing or preventing chemical species to diffuse through film insulating the substrate from the corrosive environment (7-10).

Herein we present the corrosion studies of carbon steel API 5L X65 exposed to oil production water at 50°C and 100°C, in 0.55 MPa and 10 MPa of CO₂ at stagnant, moderate and high shear stress condition. The influence of 0.001 MPa of H₂S was also investigated. By electrochemical impedance the corrosion process at metal/solution interface was monitored and evaluated during the immersion test period and weight loss test used to estimate the corrosion rate at the end of the immersion test. XRD and SEM analyses were used to characterize corrosion products, chemically and morphologically, respectively.

Experimental Procedure

All experiments were carried out in an 8L Hastelloy C-276 autoclave. The electrochemical measurements were performed in a three electrodes setup configuration cell. The working electrode was the carbon steel API 5L X65, platinum wire was used as reference electrode and the autoclave walls used as counter electrode. Working and reference electrodes were electrically insulated from the autoclave and connected to potentiostat. Three specimens of 30 mm x 20 mm x 3 mm were subjected to weight loss test and fixed to the electrically insulated autoclave hangers. The volume-to-surface ratio was 100 mL/cm². Figure 1A presents a schematic drawing of an autoclave used to stagnant tests and 1B presents the rotating cage apparatus that was adapted in the same autoclave for the dynamic tests in high shear stress. Oxygen was removed from the solution by CO₂ (99.999%) continuous bubbling, with flow rate like 200 mL/min, during 1 h/L. After that period, the solution was then transferred to the previously deaerated autoclave, which already contained the specimens. The autoclave was then conditioned to the required pressure and temperature of the tests. At this point, electrochemical data acquisition started.

Test Conditions:

- Electrolyte solution: production water containing 115,000 mg/L of Cl⁻
- Temperature: 100 °C;
- Total pressure: 0.55 MPa of CO₂ or 10 MPa, with and without 0.001 MPa of H₂S;
- Flow regime: Static, 20 Pa and 50Pa;
- Immersion time: 7 days

After the immersion test, specimens were rinsed in water and acetone several times, and then dried in warm air. The specimens were sent straight to X-ray analyses and then to SEM evaluation. After that, specimens were subjected to weight loss tests. Immersion test follow

the experimental procedures from ASTM G31 standard and for weight loss test ASTM G1 standard experimental procedures were used.

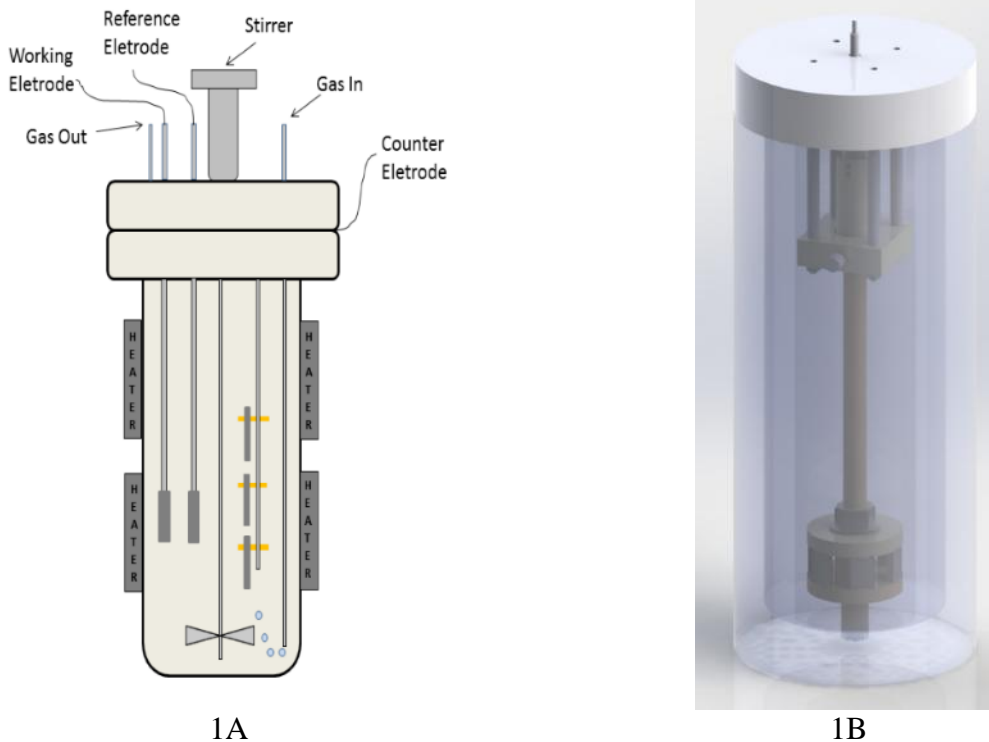


Figure 1: Schematic Autoclave and the Specimens Distribution Drawing, 1A – static tests, 1B – dynamic tests (20 Pa and 50 Pa).

Results and discussion

To evaluate the sweet corrosion of carbon steel API 5L X65 including CO₂ supercritical conditions we performed tests comprising two CO₂ pressure levels (0.55 MPa and 10 MPa) in two temperatures (50 °C and 100 °C), the electrolyte solution composition was similar to oil production water according to field analyses. Additionally, we also evaluated the effect of 0.001 MPa of H₂S and shear stress on API 5L X65 carbon steel corrosion.

Table 1 summarizes the corrosion rates, and scale structure found to all tests performed. Comparing immersion tests carried on at 50°C (T1, T3) and 100°C (T2, T4) the corrosion rates obtained showed a strong temperature influence to tests performed at 0.55 MPa whereas to tests at 10 MPa the corrosion rates decreased only slightly to tests performed at 100°C.

Table 1 – Carbon steel API 5L X65 corrosion data and scale formation

Test	Shear stress (Pa)	Temperature (°C)	P _{CO2} (MPa)	P _{H2S} (MPa)	Corrosion Rate (mm/year)	Scale (Structure)
1	0	50	0.55	-	6.6	FeCO ₃ Fe ₂ O ₂ CO ₃
2	0	100	0.55	-	1.1	FeCO ₃ Fe ₂ O ₂ CO ₃
3	0	50	10	-	4.7	FeCO ₃ Fe ₂ O ₂ CO ₃

4	0	100	10	-	3.7	FeCO ₃ Fe ₂ O ₂ CO ₃
5	0	50	10	0.001	8.0	FeS
6	0	100	10	0.001	6.1	FeCO ₃ Fe ₂ O ₂ CO ₃
7	20	100	10	-	9.2	FeCO ₃
8	20	100	10	0.001	17.8	FeCO ₃
9	50	100	10	-	13.1	FeCO ₃
10	50	100	10	0.001	41.9	FeCO ₃

The impedance diagrams and SEM images from test 1 and 2 specimens are presented on figure 2. To test 1 is possible to identify many defects in the film formed at 50 °C (fig. 2A2). The Nyquist diagrams are typical of an active CO₂ corrosion interface (fig. 2A1) (1). However, to test 2 the film morphology and impedance diagrams (fig. 2B1) are completely different and a compact film is observed. On fig. 2B2 is possible to see the siderite crystals (see figure inset). The impedance diagram shows a capacitive loop at moderate frequencies, followed by another element at lower frequencies (up to 2 mHz), probably related to diffusion effects. Zreal values are quite superior of those observed at 50°C and increase with time from 40 h of immersion. Therefore, the morphologies features observed to films formed at 50 and 100°C corroborate the results obtained by electrochemical impedance (see figure 2). Not only siderite (FeCO₃) but also orthorhombic iron carbonate (Fe₂O₂CO₃) were identified on films formed on test 1 and 2. The presence of the later may be due to siderite oxidation due to air exposure just before these analyses.

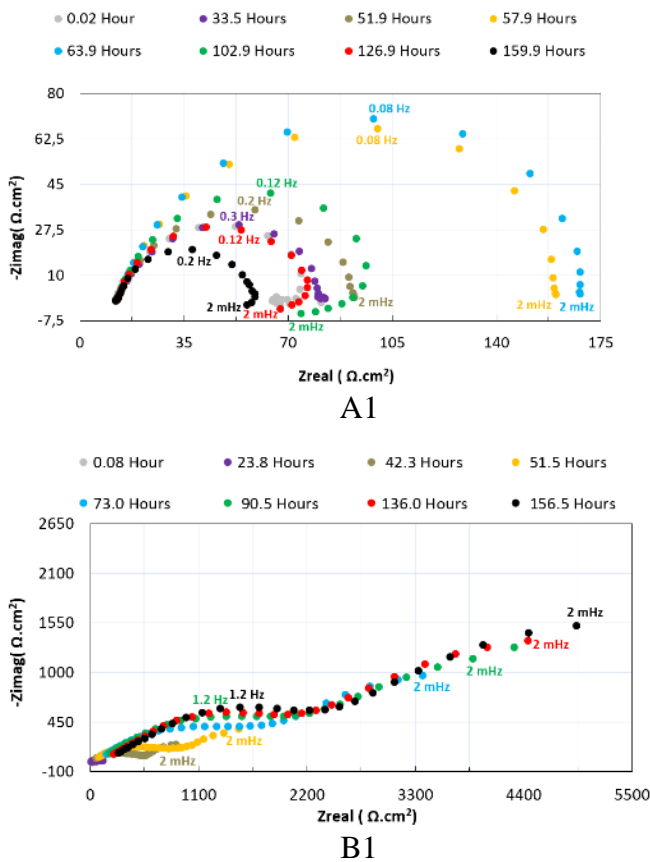


Figure 2: Nyquist diagrams and SEM to carbon steel API 5L X65 on production water, 0.55 MPa of CO₂ at 50°C (A = test 1) and 100°C (B = test 2)

On figure 3A1 and B1 the impedance diagrams to tests performed at 10 MPa show the same process observed to test at 0.55 MPa. The films morphology are also quite similar to those observed at lower CO₂ pressure, where no crystalline structure was observed on films formed at 50°C (fig 3A2) and a well-defined crystalline layer typical to FeCO₃ to the ones formed at 100°C (fig 3B2). The corrosion rates and film structure are presented on table 1. Again, the corrosion rate to tests at 100°C was lower than that observed at 50°C.

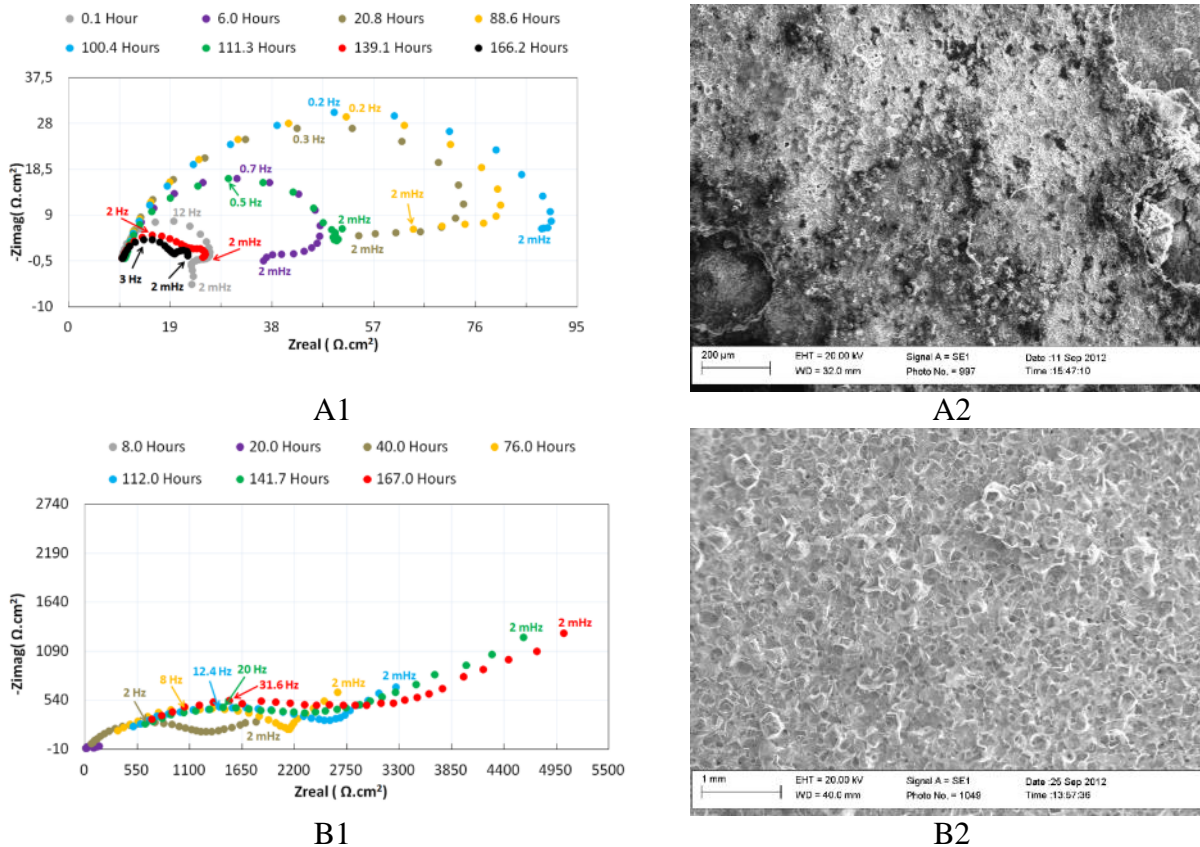


Figure 3: Nyquist diagrams and SEM to carbon steel API 5L X65 on production water, 10 MPa of CO₂ at 50°C (A = test 3) and 100°C (B = test 4)

Based on tests 5 and 6 results it is possible to infer that even small concentration of H₂S (0.001MPa) has a strong influence on X65 carbon steel corrosion. The electrochemical data to test performed at 50°C and H₂S/CO₂ 0.001/10 MPa (fig. 4 A1) showed a capacitive loop followed by an inductive element associated with carbon steel anodic dissolution (1). An irregular film was formed on steel surface, as presented in fig. 4A2. The corrosion rate found was around 40% higher than the one observed in the same conditions but in the absence of H₂S (test 3). Comparing the results presented on fig. 4A and 4B we evaluate the temperature influence on carbon steel corrosion. The corrosion rate was around 20% lower at 100°C. The same tendency observed in the absence of H₂S. The impedance diagrams (fig 4B1) are in agreement with film morphology, and at least two capacitive loops are present, probably related to film/solution and steel/solution interfaces. Despite of the well-define FeCO₃ crystalline structure, Fig 4B2 also shows some uncovered regions of carbon steel (figure inset). The films XRD analyses showed mackinawite as main film formed at 50°C and siderite + orthorhombic iron carbonate to film formed at 100°C.

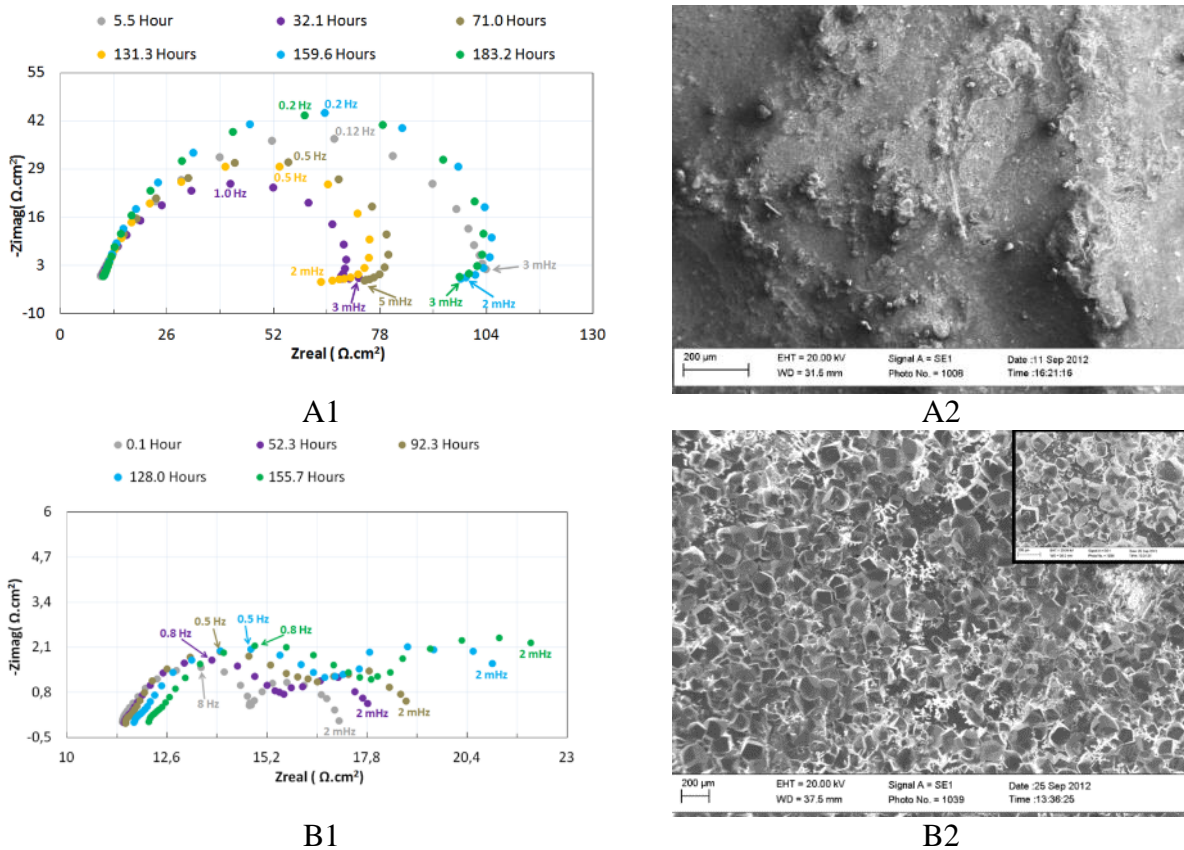


Figure 4: Nyquist diagrams and SEM to carbon steel API 5L X65 on production water, H_2S/CO_2 0.001/10 MPa at 50°C (A = test 5) and 100°C (B = test 6)

Once X65 carbon steel is widely used in oil pipelines we performed tests in dynamic conditions, simulating the shear stress caused by the oil on carbon steel pipe surface. The corrosion rates and corrosion products characterization are presented on table 1. Figure 5 show the images of specimens just after the immersion tests (fig 5A1) and after the weight loss pickling (fig 5A2).

Test 7 was carried out at 20 Pa, 10 MPa of CO_2 and 100°C. Even at that level of shear stress a crystalline layer of $FeCO_3$ was formed on steel surface. Figure 5A1 shows the carbon steel covered by siderite and figure 5A2 the specimen after the weight loss pickling. The film composition identified by XRD analyses is presented on table 1. Comparing the static test (test 4) with test performed at 20 Pa (test 7) the corrosion rate increased by a factor of 2.5. The presence of 0.001 MPa of H_2S in the same conditions yield a 2x increase on corrosion rates, from 9.2 to 17.8 mm/y, to test 7 and test 8 respectively. From images of figures 5 and 6 it is clearly that the more pronounced corrosion effects on carbon steel are in the presence of H_2S .

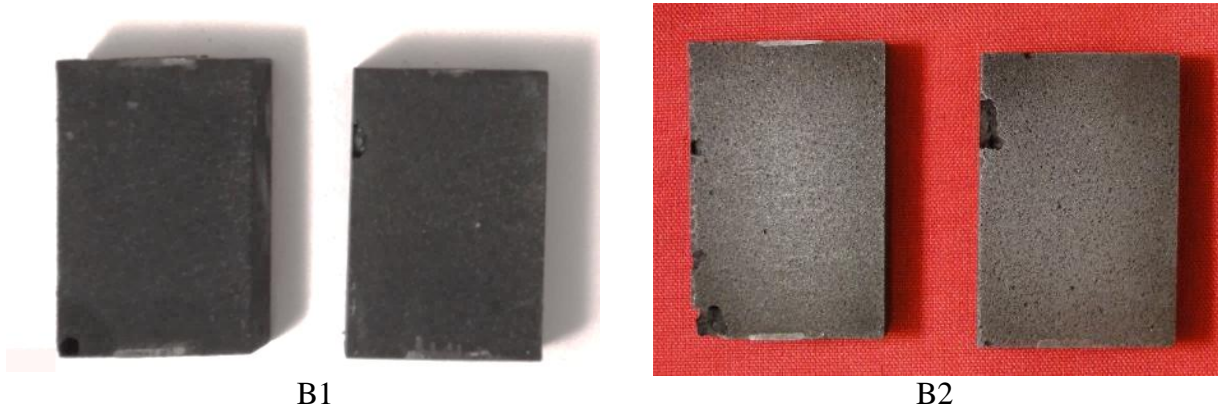


Figure 5: Images of carbon steel API 5L X65 after immersion test 7: 20 Pa of shear stress on production water, 10 MPa of CO₂ at 100°C.

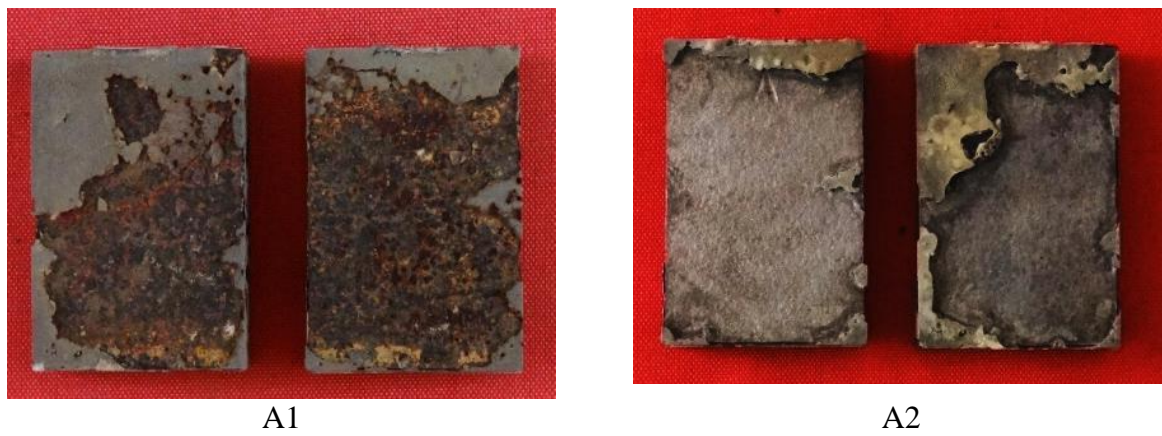


Figure 6: Images of carbon steel API 5L X65 after immersion test 8: 20 Pa of shear stress on production water, H₂S/CO₂ 0.001/10 MPa at 100°C.

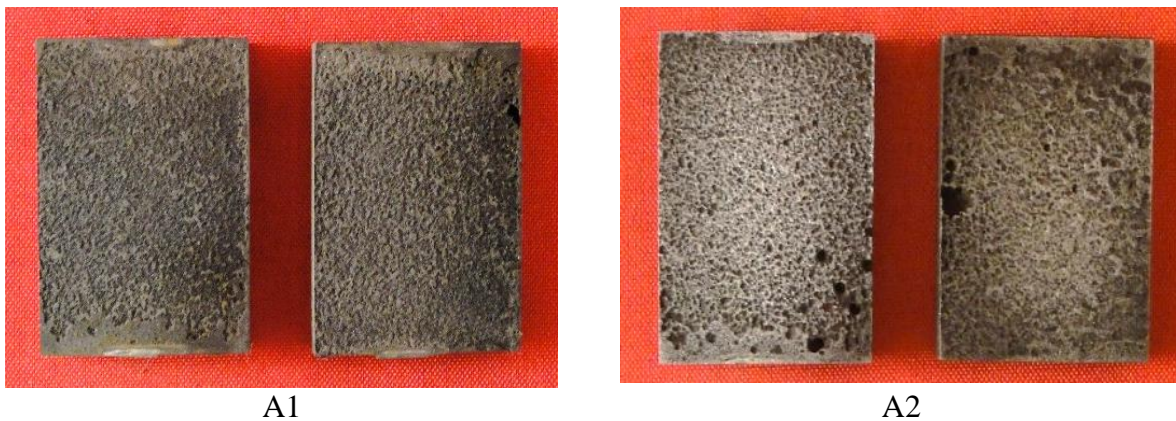


Figure 7: Images of carbon steel API 5L X65 after immersion test 9: 50 Pa of shear stress on production water, 10 MPa of CO₂ at 100°C.

As it was expected, the corrosion rate increased with shear stress. Specimen images after the test performed at 50 Pa, presented on figures 7 and 8, show a severe general corrosion to test 9 and 10. Additionally, at 50 Pa the H₂S addition increased remarkably the corrosion rate, from 17.8 mm/y to 41.9 mm/y, to test 9 and 10 respectively.

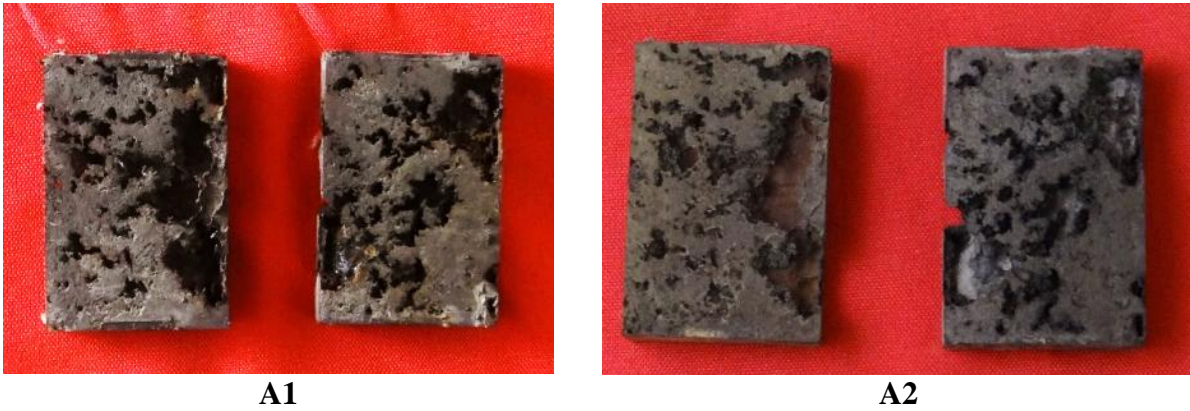


Figure 8: Images of carbon steel API 5L X65 after immersion test 10: 50 Pa of shear stress on production water, H₂S/CO₂ 0.001/10 MPa at 100°C.

Figure 9 summarizes the results presented herein. The temperature influence was more evident on tests performed at 0.55 MPa of CO₂. These results indicate that the Siderite film formed at 100°C 0.55 MPa of CO₂ at static conditions decreased considerably the corrosion kinetics.

At higher pressure, 10 MPa, such a pronounced temperature effect was not present. Still on static conditions, an addition of 0.001 MPa of H₂S increased the corrosion rate in roughly 60% but values observed to tests performed at 100°C were slightly lower than at 50°C.

The impedance diagrams and SEM images of films formed in the presence of 0.01% of H₂S, despite the fact of its crystalline structure, the electrolyte is able to permeate through it reaching the carbon steel surface, once the film is not covering the entire surface.

The shear stress had a strong impact on corrosion rate, and almost a linear increase observed in the presence of H₂S.

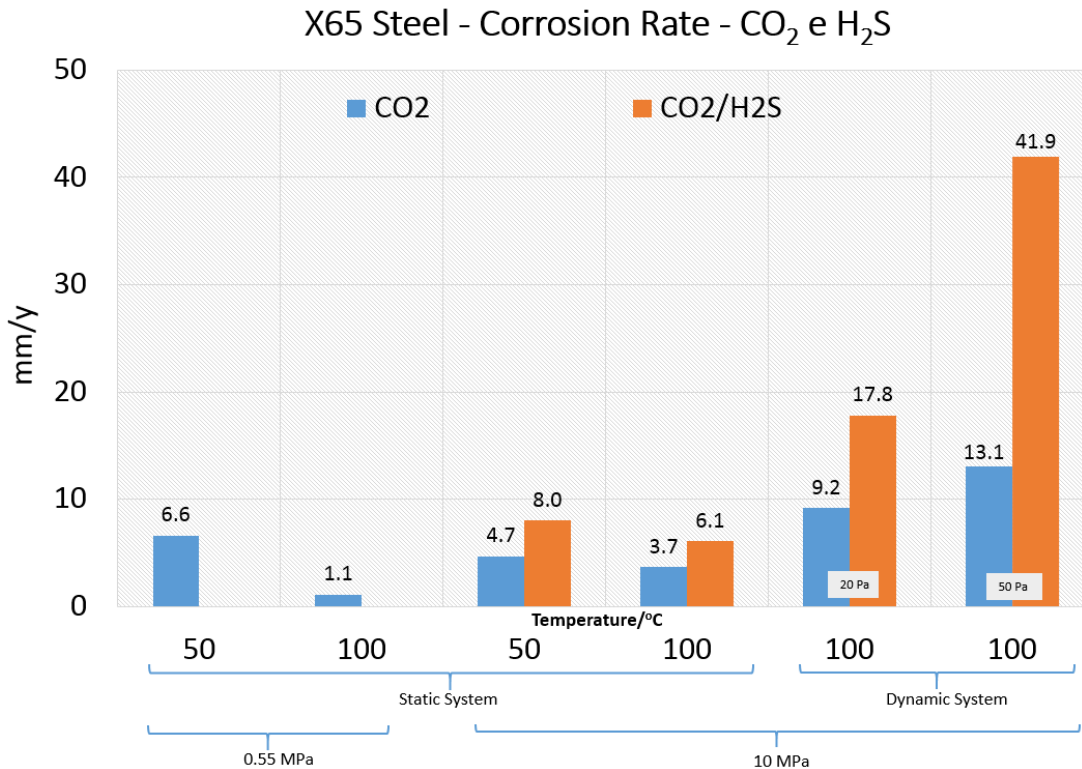


Figure 9: Carbon steel API 5L X65 corrosion rates on production water (115,000 mg/L Cl)

Conclusions

Based on the results presented in this paper is possible to conclude that:

- Formation of a crystalline and compact film of siderite can decrease the carbon steel X65 corrosion rate considerably at 0.55 MPa but only slightly at 10 MPa;
- Presence of 0.01% of H₂S in the gas phase was responsible for at least 50% increase on corrosion rates obtained by weight loss tests;
- H₂S negative impact on corrosion rate emphasizes its influence on siderite formation even at low concentration;
- 0.01% of H₂S in the gas phase was not enough to prevent the siderite formation at 100°C but the film formed was less compact and allowed electrolyte permeation.

References

- 1 – ALMEIDA, T. C., BANDEIRA, M. C. E., MOREIRA, M. M., MATTOS, O. R., The Role of CO₂ on Carbon Steel Corrosion. Corrosion 2015, Houston, paper 2015-5807.
- 2 – REMITA, E., TRIBOLLET, B., SUTTER, E., VIVIER, V., ROPITAL, F., KITTEL, J., Hydrogen evolution in aqueous solutions containing dissolved CO₂: Quantitative contribution of the buffering effect, Corrosion Science, Oxford, Vol. 50, N. 5, p.1433-1440, 2008.
- 3 - LI DA-PENG, ZHANG L., YANG, JIAN-WEI, LU MIN-XU, DING JIN-HUI, LIU MING-LIANG, Effect of H₂S concentration on the corrosion behavior of pipeline steel under the coexistence of H₂S and CO₂, International Journal of Minerals, Metallurgy and Materials, Vol. 21, N. 4, Page 388, April 2014.
- 4 – SMITH, S. N., JOOSTEN, M. W., Corrosion of carbon steel by H₂S in CO₂ containing oilfield environments, Corrosion 2006, Houston, paper 2015-0115.
- 5 – BROWN, B., PARAKALA, S. R., NESIC, S., CO₂ Corrosion in the presence of trace amounts of H₂S, Corrosion 2004, Houston, paper 2004-0736.
- 6 – SUHOR, M. F., MOHRAMED, M. F., MUHAMMAD NOR, A., SINGER, M., NESIC, S., Corrosion of Mild Steel in High CO₂ Environment: Effect of the FeCO₃ Layer”, Corrosion 2012, Houston, paper 2012-1434.
- 7 – SUN, J. B., ZANG, G. A., LIU, W., LU, M. X., The Formation Mechanism of Corrosion Scale and Electrochemical Characteristic of Low Alloy Steel in Carbon Dioxide-saturated solution, Corrosion Science, Oxford, Vol. 57, p. 131-138, 2012.
- 8 – ZHANG, Y., PANG, X., QU, S., LI, X., Gao, K., Discussion of the CO₂ Corrosion Mechanism Between Low Partial and Supercritical Condition, Corrosion Science, Oxford, Vol.59, p. 186-197, 2012.
- 9 – SKAR, J. I., ANDERSON, T. R., BAPTISTA, I. P., GUEDES, F. M., HENRIQUES, C. C. D., MOREIRA, R. M., CO₂/H₂S Corrosion Prediction – Laboratory Testing and Interpretation of Data, Corrosion 2012, Houston, paper 2012-1522.
- 10 – LEE, K. J., NESIC, S., The Effect of Trace Amount of H₂S on CO₂ Corrosion Investigated by Using the EIS Technique, Corrosion 2005, Houston, paper 2005-0630.